Arabian Journal of Chemistry (2016) 9, 596–605

King Saud University

Arabian Journal of Chemistry

www.ksu.edu.sa
www.sciencedirect.com

ORIGINAL ARTICLE

Synthesis, spectral characterisation, morphology, biological activity and DNA cleavage studies of metal complexes with chromone Schiff base

P. Kavitha, K. Laxma Reddy *

Department of Chemistry, National Institute of Technology, Warangal 506004, Andhra Pradesh, India

Received 11 June 2012; accepted 4 September 2012
Available online 11 September 2012

KEYWORDS

2-Amino pyridine;
3-Formyl chromone;
Antimicrobial activity;
DNA cleavage;
Nematicidal activity

Abstract Cu(II), Co(II), Ni(II) and Zn(II) complexes have been synthesized using 3-((pyridine-2-ylimino)methyl)-4H-chromen-4-one as a ligand derived from 3-formyl chromone and 2-amino pyridine. All the complexes were characterised by analytical, conductivity, IR, electronic, magnetic, ESR, thermal, powder XRD and SEM studies. The analytical data revealed that the metal to ligand molar ratio is 1:2 in all the complexes. Molar conductivity data indicates that all the complexes are neutral in nature. On the basis of magnetic and electronic spectral data, octahedral geometry is proposed for all the complexes. Thermal behaviour of the synthesized complexes indicates the coordinated and lattice water molecules are present in the complexes. The X-ray diffraction data suggest a triclinic system for all compounds. Different surface morphologies were identified from SEM micrographs. All metal complexes exhibit fluorescence. The antimicrobial and nematicidal activity data show that metal complexes are more potent than the parent ligand. The DNA cleavage activity of the ligand and its metal complexes were observed in the presence of H_2O_2.

1. Introduction

Amino pyridines are widely used in pharmacological and medical applications (Okamato et al., 1997; Dega-Szafran et al., 1994; Carmona et al., 1993). 2-Aminopyridine serves as a useful chelating ligand in a variety of inorganic and organometallic applications (Suksrichavalit et al., 2009; Fuhrmann et al., 1996; McWhinnie, 1964). Chromones are a group of naturally occurring compounds which are ubiquitous in nature especially in plants (Ya Sosnovskikh, 2003; Ellis, 1977). Chromone derivatives have been of special interest due to their biological activities including antimycobacterial, antifungal, antiviral, antiallergenic, antihypertensive, anticonvulsant, antimicrobial, anticancer, antioxidant, anti-inflammatory, protein kinase C inhibitors and mushroom tyrosinase inhibition activities (Athanasellis et al., 2006; Singh et al., 2002a; Piao et al., 2002; Barve et al., 2006; Walenzyk et al. 2005). Chromone derivatives and their metal complexes also act as good fluorescent compounds. The design and synthesis of brightly emissive molecules, having a heterocyclic back bone and allowing for alterations in emission properties is a subject of current

* Corresponding author. Tel.: +91 870 2462650; fax: +91 870 2459547.
E-mail address: laxmareddychem12@gmail.com (K. Laxma Reddy).
Peer review under responsibility of King Saud University.

ELSEVIER Production and hosting by Elsevier

http://dx.doi.org/10.1016/j.arabjc.2012.09.001

research in view of their potential applications as chemo sensors and optoelectronic devices etc. (Teimouri, 2011; Wang et al., 2009). In recent years, the interaction of transition metal complexes with DNA has been extensively studied for their usage as probes for DNA structure and their potential application in chemotherapy. One of the most important DNA related activity of the transition metal complexes is that, some of the complexes show the ability to cleave DNA. Very recently, Cu(II) complexes have been reported to be active in DNA strand scission (Liu et al., 2002; Vaidyanathan and Nair, 2003; Reddy et al., 2006). A huge number of literature reports are available on the DNA binding studies of formyl chromone Schiff bases and their metal complexes (Li et al., 2010a; Wang et al., 2009; Qin et al., 2007). Knowledge of DNA binding parameters of these molecules explores their potential applications, since their binding mode could be associated with their ability to cause DNA damage (Ng et al., 2000; Sancar and Sancar, 1988; David and Williams, 1998). Further, DNA damage is leading to the inhibition of uncontrolled growth of cancerous cells. Schiff base metal complexes also act as active nematicidal agents (Jain et al., 2004).

Keeping the above literature in view, we have undertaken the synthesis and structural characterization, morphological, fluorescence and biological activity studies of Cu(II), Co(II), Ni(II) and Zn(II) complexes with 3-((pyridine-2-ylimino)methyl)-4H-chromen-4-one as ligand. Emphasis has been put on biological evaluation of the complexes.

2. Experimental

2.1. Materials

AR grade 2-hydroxy acetophenone, phosphorous oxychloride, dimethyl formamide, 2-amino pyridine, cobalt acetate, copper acetate, nickel acetate, zinc acetate and solvents used were procured from Merck.

2.2. Synthesis of ligand (L)

The synthesis of the ligand was carried out by stirring the mixture of 3-formyl chromone (1 mM) (Nohara et al., 1973) with 2-amino pyridine (1 mM) in methanol at 40–50 °C. The light yellow precipitate was filtered off, and washed several times with methanol and recrystallized from methanol and finally dried in vacuo desiccators over anhydrous $CaCl_2$ (Yield: 90%). The experimental details were presented in Scheme 1.

2.3. Synthesis of metal complexes

A hot methanolic solution of the respective metal acetate (Cu(II), Co(II), Ni(II) and Zn(II)) (1 mM) was added to the hot methanolic solution of ligand (L) (2 mM). The mixed solution was stirred at room temperature for 1 h 30 min. The precipitates thus separated out, were washed with methanol and dried in vacuo.

2.4. Physical measurements

Elemental analysis for C, H, and N was performed using Perkin Elmer CHN analyser. Molar conductance of the complexes was measured in DMF using Digisun conductivity meter. Thermogravimetric measurements were recorded on TA instruments (SDT 200) at a heating rate of 20 °C and a nitrogen flow rate of 20 ml/min. Room temperature magnetic measurements were carried out on a Guoy balance by making diamagnetic corrections using Pascal's constant. The IR spectra (4000–400 cm^{-1}) in KBr discs were recorded on TENSOR 2 spectrophotometer. The UV–vis spectra of the ligand and its metal complexes were performed using Analytikzena Specord 205 spectrophotometer. The solid state ESR spectrum of the Cu(II) complex was recorded using Bruker EMX EPR spectrometer operating at X-band frequencies having a 100 kHz field modulation at room temperature. Fluorescence spectra were recorded using Perkin Elmer LS 55 fluorescence spectrometer. The X-ray powder diffraction analysis was carried out by using Xpert-Pro X-ray diffractometer using Cu-Kα (1.5360 Å) radiation. Scanning electron microscopy (SEM) of the complexes was obtained in a Hitachi S-520 electron microscope at an accelerated voltage of 10 kV.

2.5. In vitro antimicrobial studies

In vitro anti bacterial and anti fungal activities of the ligand and its complexes were tested against bacterial species *Proteus vulgaris, Staphylococcus aureus*, *Klebsiella pnuemoniae*, *Bacillus subtilis* fungal species *Candida albicans* by the disc diffusion method. Nutrient agar plate was evenly spread by using a sterile glass spreader. Sterile antibiotic discs (6 mm in diameter, prepared using Whatman No. 1 paper) were placed over the medium. To determine the antimicrobial activity, 100 μg of the compounds (initially dissolved in DMSO) was transferred to each disc with the help of a micropipette, simultaneously maintaining standard kanamycin (30 μg/disc) against bacteria and Clotrimazole (10 μg/disc) for fungi. After overnight incubation at 37 °C for bacteria and 25 °C, the zone of inhibition was measured in 'mm' and compared with standard antibiotics. Control measurements were carried out with DMSO. All the experiments were performed in triplicates and the average zones of inhibition were recorded. Minimum inhibitory concentration (MIC) of all the compounds was determined by using serial dilution method.

2.6. Nematicidal activity

Nematicidal activity was carried out on *Meloidogyne incognita*. Nematode *M. Incognita* is known to attack more than 3000

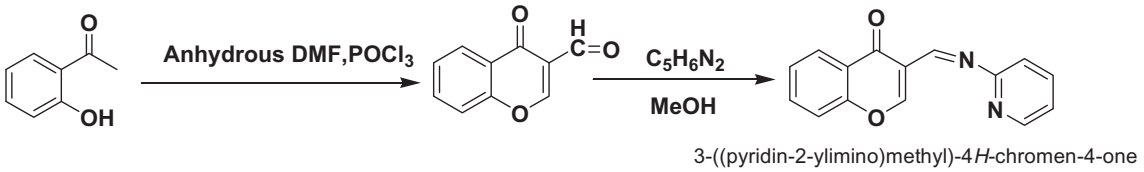

3-((pyridin-2-ylimino)methyl)-4*H*-chromen-4-one

Scheme 1 Schematic representation of synthesis of ligand.

host plants (Parvatha and Khan, 1991). The yields of okra, tomato, and brinjal typically suffer 90.9%, 46.2%, and 2.3% losses, respectively due to *M. incognita*. *Meloidogyne incognita* produces galls on the roots of many host plants and is responsible for a 44.87% yield loss in brinjal. The root-knot nematode produces galls on the roots of many vegetables, pulses, some fruit crops, tobacco, and ornamental crops and causes severe losses (Kapoor et al., 2012).

2.6.1. Culture preparation

Fresh egg masses of *Meloidogyne incognita* were collected from stock culture maintained on tomato (*Lycopersicon esculentum*) root tissues and kept in water for egg hatching. The eggs suspension was poured on a cotton wool filter paper and incubated at 28 ± 2 °C to obtain freshly hatched juveniles (J2). Juveniles collected within 48 h were used for screening the nematicidal activity of the compounds.

2.6.2. Mortality test

The ligands and their complexes were initially dissolved in dimethyl sulfoxide (DMSO) and then in distilled water to make dilutions of 250, 150 and 50 μg/ml. Experiments were performed under laboratory conditions at 28 ± 2 °C. About 100 freshly hatched second stage juveniles were suspended in 5 ml of each diluted compound and incubated. Distilled water with nematode larvae was taken as the control. The dead nematodes were observed under an inverted binocular microscope. After an incubation of 24 and 48 h, percentage of mortality was calculated. Nematodes were considered dead, if they did not move when probed with a fine needle (Cayrol et al., 1989).

2.7. Agarose gel electrophoresis

Agarose gel electrophoresis was used to study the DNA cleavage activity of the ligand and its metal complexes. pUC19 plasmid was cultured, isolated and used as DNA for the experiment. Test samples (1 mg/ml) were prepared in DMF. 25 μg of the test samples and 5 μl of H_2O_2 (500 μM) were added to the isolated plasmid and incubated for 2 h at 37 °C. After incubation, 30 μl of plasmid DNA sample mixed with bromophenol blue dye was loaded into the electrophoresis chamber wells along with the control (plasmid DNA in DMF without test sample) and standard DNA marker. Finally, it was loaded onto agarose gel and electrophoresed at a constant voltage of 50 V for 30 min. After the run, gel was removed and stained with 10.01 μg/ml ethidium bromide and image was taken in Versadoc (Bio-Rad) imaging system. The results were compared with the standard DNA marker. The same procedure was followed in the absence of the oxidising agent (H_2O_2) also.

3. Results and discussion

The analytical data and physical properties of the ligand and its complexes are listed in Table 1. The Schiff base ligand (L) is soluble in common organic solvents. The resultant Schiff base complexes are partially soluble in MeOH and $CHCl_3$ but freely soluble in DMF and DMSO. The analytical data indicate that the metal to ligand ratio is 1:2 in all the complexes. The conductivity data of all the metal complexes indicates that all are neutral in nature (Geary, 1971).

3.1. IR spectral data

Infrared spectral data of ligand and its metal complexes are listed in Table 2. In the IR spectra of ligand (L) appearance

Table 2 IR spectral data of ligand and its metal complexes.

Compound	υ(O–H)	υ(C=N)	υ(C=O)	υ(M–N)	υ(M–O)
L		1596	1654		
$[Cu(L)_2(H_2O)_2]$	3442 838	1576	1601	454	527
$[Co(L)_2(H_2O)_2]$	3427 867	1580	1627	487	584
$[Ni(L)_2(H_2O)_2]$	3425 848	1580	1629	487	593
$[Zn(L)_2(H_2O)_2]\cdot 2H_2O$	3441 846	1581	1630	467	577

Table 1 Physical and analytical data of the ligand and its metal complexes.

Compound (formula weight)	Colour (%yield)	MP (°C)	% Found (cald)				Molar conductance (ohm^{-1} cm^2 mol^{-1})
			C	H	N	M	
L $C_{15}O_2N_2H_{10}$ (250)	Light yellow (90)	210	72.26 (72.00)	4.05 (4.00)	11.15 (11.20)	–	
$[Cu(L)_2(H_2O)_2]$ $[Cu(C_{15}O_2N_2H_1)_2(H_2O)_2]$ (599.5)	Leaf green (80)	218	(60.00) (60.05)	(4.06) (4.00)	(9.25) (9.34)	(10.60) (10.59)	12
$[Co(L)_2(H_2O)_2]$ $[Co(C_{15}O_2N_2H_{10})_2(H_2O)_2]$ (594.9)	Lemon yellow (82)	282	(60.49) (60.51)	(4.00) (4.03)	(9.45) (9.41)	(9.99) (9.90)	13
$[Ni(L)_2(H_2O)_2]$ $[Ni(C_{15}O_2N_2H_{10})_2(H_2O)_2]$ (594.7)	Light green (75)	> 300	(60.43) (60.53)	(4.05) (4.03)	(9.55) (9.41)	(9.80) (9.87)	14
$[Zn(L)_2(H_2O)_2]\cdot 2H_2O$ $[Zn(C_{15}O_2N_2H_{10})_2(H_2O)_2]\cdot 2H_2O$ (637.4)	Yellow (74)	> 300	(56.50) (56.47)	(4.45) (4.39)	(8.70) (8.78)	(10.36) (10.26)	11

of a band at 1654 cm^{-1}, assignable to the υ(C═O) of chromone group, showed a shift to 24–53 cm^{-1} to a lower wavenumber in its complexes, indicating the participation of oxygen of the carbonyl group in coordination to the metal ion (Li et al., 2010b). The most characteristic band of the Schiff base ligand that appeared at 1596 cm^{-1} is due to υ(C═N) of azomethane group that underwent a shift to 15–20 cm^{-1} to lower wavenumber side in all the metal complexes, indicating that the involvement of the nitrogen of (C═N) group in coordination to the metal ion (Aazam et al., 2012). All the metal complexes showed a broad band in the range of 3500–3400 cm^{-1}, followed by another band at 810–870 cm^{-1} that suggests the presence of water molecules in the metal complexes (Singh et al., 2002b; Shukla et al., 1983). Participation of oxygen and nitrogen atoms in coordination is further confirmed by far IR spectral bands in the range of 600–400 cm^{-1} corresponding to υ(M–N) and υ(M−O), respectively.

3.2. Electronic and magnetic moment data

The electronic spectra of Cu(II), Co(II), Ni(II) and Zn(II) complexes are given in Fig. 1. The electronic spectral data along with the various ligand field parameters and magnetic moment values are depicted in Table 3. The ligand showed two bands in its electronic spectra at 33898 and 27027 cm^{-1} corresponding to the $\pi \rightarrow \pi^*$ and $n \rightarrow \pi^*$ transitions, respectively. The electronic spectra of Cu(II) complex exhibits three bands at 11,235, 14,619 and 22,000 cm^{-1} are assigned to $^2B_{1g} \rightarrow {}^2B_{2g}$, $^2B_{1g} \rightarrow {}^2E_g$ and LMCT transitions, respectively. These bands are characteristic for distorted octahedral geometry. The magnetic moment value 1.75 BM also confirms that it is in distorted octahedral geometry (Raman et al., 2004). The electronic spectra of Co(II) complex that exhibit three bands at 8,500, 14,450 and 19,000 cm^{-1} are assignable to $^4T_{1g}$ (F) → ^{4}T2g (F) (ν_1), $^4T_{1g}$ (F) → $^4A_{2g}$ (F) (ν_2) and $^4T_{1g}$ (F) → $^4T_{1g}$ (P) (ν_3) transitions, respectively, characteristic of octahedral geometry. The magnetic moment value (3.92 BM) obtained for Co(II) complex also confirms the octahedral geometry. The electronic spectra of Ni(II) complex is consistent with octahedral geometry showing three bands at 9,400, 15,980 and 24,200 cm^{-1} assignable to the $^3A_{2g}$ (F) → $^3T_{2g}$ (F) (ν_1), $^3A_{2g}$ (F) → $^3T_{1g}$ (F) (ν_2) and $^3A_{2g}$ (F) → $^3T_{1g}$ (P) (ν_3) transitions, respectively characteristic of octahedral geometry. The magnetic moment value (3.15 BM) also confirms the octahedral geometry of Ni(II) complex. Since Zn(II) is a d^{10} metal ion no band is expected in the visible region and is also found as a diamagnetic complex, as expected. However, a strong band observed at 28,169 cm^{-1} is assignable to the metal to ligand charge transfer transition.

3.3. ESR spectra

The ESR spectrum of Cu(II) complex has been recorded at room temperature and is given in Fig. 2. In the present study

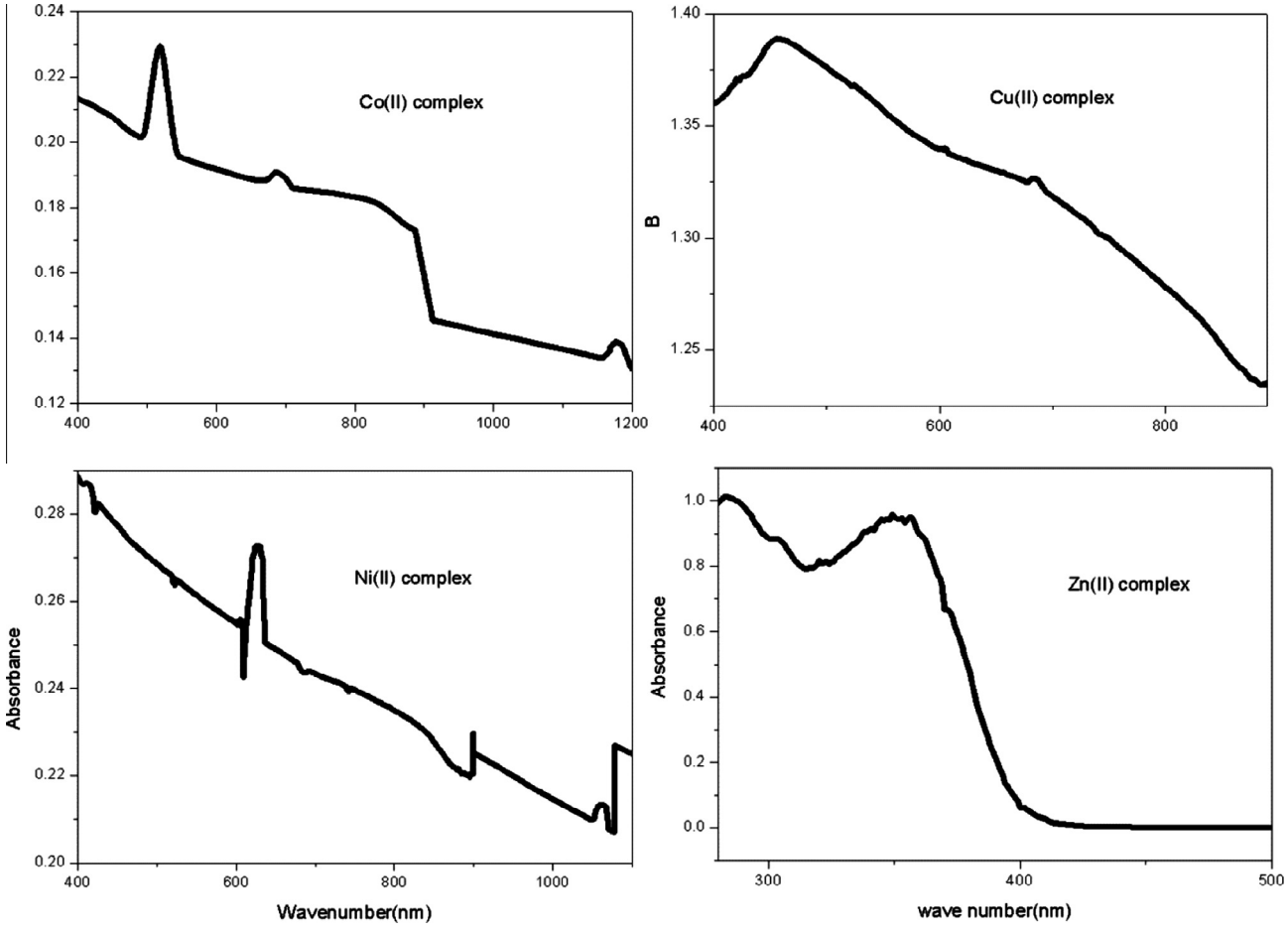

Figure 1 Electronic spectra of Cu(II), Co(II), Ni(II) and Zn(II) complexes.

Table 3 Electronic spectral data and magnetic moment values of metal complexes.

Compound	Band position (cm^{-1})	Assignment	Ligand field parameters			μ_{eff} (B.M)
			Dq	B	β	
$[Cu(L)_2(H_2O)_2]$	11,235	$^2B_{1g} \rightarrow {}^2E_g$	–	–	–	1.75
	14,619	$^2B_{1g} \rightarrow {}^2B_{2g}$				
	22,000	LMCT				
$[Co(L)_2(H_2O)_2]$	8500	$^4T_{1g}$ (F) $\rightarrow {}^4T_{2g}$ (F) (ν_1)	595	530	0.47	3.92
	14,450	$^4T_{1g}$ (F) $\rightarrow {}^4A_{2g}$ (F) (ν_2)				
	19,000	$^4T_{1g}$ (F) $\rightarrow {}^4T_{1g}$ (P) (ν_3)				
$[Ni(L)_2(H_2O)_2]$	9400	$^3A_{2g}$ (F) $\rightarrow {}^3T_{2g}$ (F) (ν_1)	940	799	0.76	3.15
	15,980	$^3A_{2g}$ (F) $\rightarrow {}^3T_{1g}$ (F) (ν_2)				
	24,200	$^3A_{2g}$ (F) $\rightarrow {}^3T_{1g}$ (P) (ν_3)				
$[Zn(L)_2(H_2O)_2]\cdot 2H_2O$	28,169	Charge transfer	–	–	–	Diamagnetic

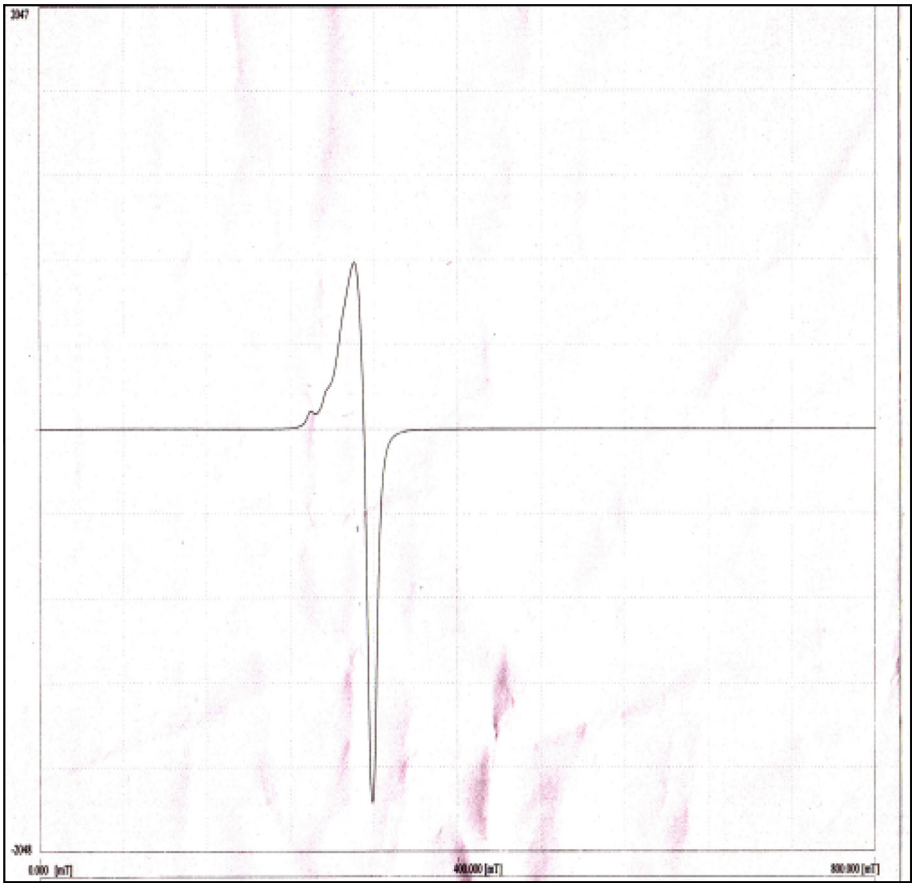

Figure 2 ESR spectra of Cu(II) complex.

Cu(II) complex shows four well resolved hyperfine peaks with the spin Hamiltonian parameters $g_{||} = 2.2921$, $g_{\perp} = 2.0704$ and $A_{||} = 143 \times 10^{-4}\,cm^{-1}$, $A_{\perp} = 34 \times 10^{-4}\,cm^{-1}$. Where, $g_{||} > g_{\perp} > 2.0023$ indicating that the unpaired electron in the ground state of Cu(II) predominately lies in $d_{x^2-y^2}$ orbital (Singh et al., 2005). The ratio of $g_{||}/A_{||}$ values also indicates the stereochemistry of the Cu(II) complexes. The range reported for square planar complexes is 105–135 cm^{-1} and for tetragonally distorted octahedral complexes is >135–250 cm^{-1}. The present Cu(II) complex has ($g_{||}/A_{||} =$ 160.28 cm^{-1}), which lies in the range reported for tetragonally distorted octahedral Cu(II) complexes (Nickless et al., 1983). Kivelson and Neiman showed that for an ionic environment $g_{||}$ is normally 2.3 or larger, but for covalent environment $g_{||}$ is less than 2.3. In the present study, $g_{||}$ value for the Cu(II) complex is 2.2921, consequently the environment is covalent. Molecular orbital coefficient α^2 (a measure of the covalency of the in-plane σ-bonding between a copper 3d orbital and the ligand orbital) was calculated by using the following equation (Kivelson and Neiman, 1961);

$$\alpha^2 = \left(\frac{A_{||}}{0.036}\right) + (g_{||} - 2.0023) + \frac{3}{7}(g_{\perp} - 2.0023) + 0.04$$

In the present study the α^2 value found to be 0.76 suggests the covalent character. The orbital reduction parameters $K_{||}$, $K_{\perp}$ and K were calculated from the following expressions (Lu et al., 1996; Solomon et al. 1992);

$$K_{||} = \frac{(g_{||} - 2.0023)\Delta E_{xy}}{8\lambda_0}, \quad K_{\perp} = \frac{(g_{\perp} - 2.0023)\Delta E_{xz}}{2\lambda_0}$$

$$K = \frac{K_{||}^2 + 2K_{\perp}^2}{3}$$

Here, the ΔE_{xy} and ΔE_{xz} corresponds to the transitions of $^2B_{1g} \rightarrow {}^2B_{2g}$ and $^2B_{1g} \rightarrow {}^2E_g$, respectively. λ_0 is the spin orbit coupling constant of free Cu(II) ion, its value is ($-828\ cm^{-1}$). In the present investigations, $K_{||}$, $K_{\perp}$ and K values of Cu(II) complex are 0.50, 0.60 and 0.57, respectively. These K values (0.52–0.68) also further confirm the covalent nature of the metal–ligand bond. Another bonding parameter G is calculated from the following expression;

$$G = \frac{g_{||} - 2.0023}{g_{\perp} - 2.0023} = \frac{4K_{||}^2 \Delta E_{xz}}{K_{\perp}^2 \Delta E_{xy}}$$

According to Hathaway (Hathaway and Billing, 1970; Hathaway, 1984), if the value of G is greater than 4, the exchange interaction between Cu(II) centres in the solid state is negligible. Whereas its values are less than 4, a considerable exchange interaction exists in the solid complex. The G values obtained in the present Cu(II) complexes are greater than 4, indicating the absence of exchange interaction between Cu(II) centres in the solid state. The values obtained for hyperfine splitting and covalency parameters are in good agreement with other Cu(II) complexes reported in the literature.

3.4. Thermal data

The decomposition stages, temperature range, decomposition products, as well as the found and calculated mass loss percentages of all the complexes are illustrated in Table 4. The TG curve of Co(II) complex is shown in Fig. 3. All these complexes follow the same pattern of thermal decomposition.

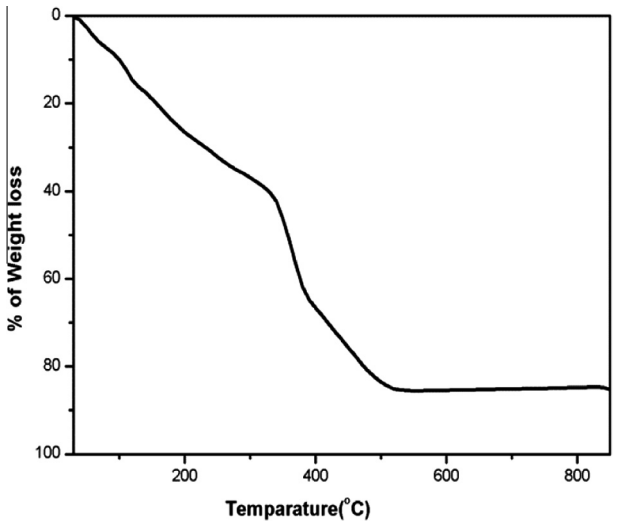

Figure 3 TG graph of Co(II) complex.

$[Cu(L)_2(H_2O)_2]$ complex was decomposed in three stages. The first step corresponds to the loss of two coordinated water molecules in the temperature range between 30–241 °C with a mass loss of 6.38%. In the second and third steps, the total loss of ligand molecules was observed in the temperature range between 242–347 and 348–453 °C with a mass loss of 53.80% and 26.46%, respectively. The final mass loss 13.36% is due to the CuO as residue.

$[Co(L)_2(H_2O)_2]$ complex was decomposed in three steps. The first step occurrs within the temperature range of 30–320 °C and can be attributed to the loss of two coordinated water molecules and a ligand molecule. The second and third steps correspond to the complete loss of the ligand molecule in the temperature range between 321–400 and 401–560 °C with a mass loss of 26.73% and 15.59%, respectively. The remaining mass loss 12.48% is due to the formation of CoO as residue.

$[Ni(L)_2(H_2O)_2]$ complex was decomposed in three steps. The first step corresponds to the loss of two coordinated water

Table 4 Thermal data of metal complexes.

Complex	Temperature (°C)	Weight loss found (cald%)	Assignment
$[Cu(L)_2(H_2O)_2]$	30–241	6.38 (6.00)	$2H_2O$
$[Cu(C_{15}O_2N_2H_{10})_2(H_2O)_2]$	242–347	53.80 (54.38)	$C_{15}ON_2H_{10} + C_5N_2H_4$
	348–453	26.46 (26.35)	$C_{10}O_2H_6$
	> 453	13.36 (13.27)	CuO (residue)
$[Co(L)_2(H_2O)_2]$	30–320	45.20 (45.38)	$2H_2O + C_{15}ON_2H_{10}$
$[Co(C_{15}O_2N_2H_{10})_2(H_2O)_2]$	321–400	26.73 (26.56)	$C_{10}O_2H_6$
	401–560	15.59 (15.47)	$C_5N_2H_4$
	> 560	12.48 (12.59)	CoO (residue)
$[Ni(L)_2(H_2O)_2]$	30–198	6.09 (6.05)	$2H_2O$
$[Ni(C_{15}O_2N_2H_{10})_2(H_2O)_2]$	199–452	41.72 (42.04)	$C_{15}O_2N_2H_{10}$
	453–790	39.71 (39.35)	$C_{10}OH_6 + C_5N_2H_4$
	> 790	12.48 (12.56)	NiO (residue)
$[Zn(L)_2(H_2O)_2]\cdot 2H_2O$	30–80	6.10 (5.65)	$2H_2O + C_5N_2H_4$
$[Zn(C_{15}O_2N_2H_{10})_2\ (H_2O)_2]\cdot 2H_2O$	81–210	20.15 (20.08)	$C_5N_2H_4$
	211–420	14.35 (14.43)	$C_{10}O_2H_6 + C_{10}OH_6$
	421–890	46.99 (47.07)	ZnO (residue)
	> 890	12.41 (12.77)	

molecules with a mass loss of 6.09% in the range below 198 °C. The second and third steps correspond to the loss of ligand molecules within the temperature range of 199–452 and 453–790 °C with a mass loss of 41.72% and 39.71%, respectively. The residue with a mass loss of 12.48% is regarded as NiO.

$[Zn(L)_2(H_2O)_2]\cdot 2H_2O$ complex decomposed in four steps. The first step is due to the loss of two lattice water molecules below 80 °C with a mass loss of 6.10%. The second step correspondsto the loss of two coordinated water molecules and part of the ligand molecule in the range between 81 and 210 °C with a mass loss of 20.15%. The third and fourth steps are found in the temperature range of 211–420 and 421–890 °C with a mass loss of 14.35 and 46.99%, respectively due to the loss of ligands. The remaining mass loss 12.41% is regarded as ZnO.

Based on the above results, the proposed structures of all the metal complexes have been shown in Fig. 4.

3.5. Fluorescence studies

The emission spectra of ligand (L) and its metal complexes were studied in DMSO. The fluorescence spectra of Co(II) complex were shown in Fig. 5. The ligand (L) does not exhibit significant emission. The Cu(II) complex was characterised by emission bands at 480, 580 and 660 nm upon photo excitation at 346 nm. Co(II) complex was characterised by emission bands around 481, 690 and 745 nm upon photo excitation at 346 nm. The Ni(II) complex shows two emission bands at 457 and 638 nm (weak emission band). The Zn(II) complex exhibits a broad emission band at 470 nm upon photo excitation at 353 nm. It is important to note here that fluorescence enhancement is due to complexation of ligand with metal ion (Ghosh et al., 2011).

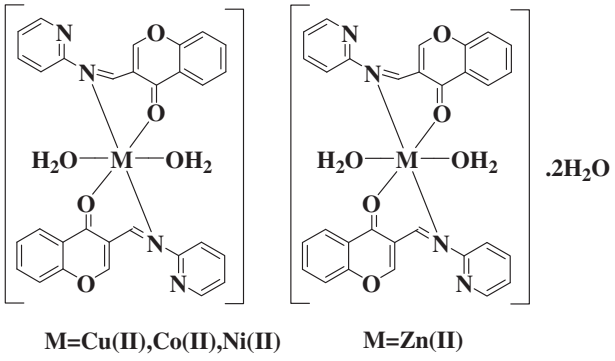

Figure 4 Proposed structures for all metal complexes.

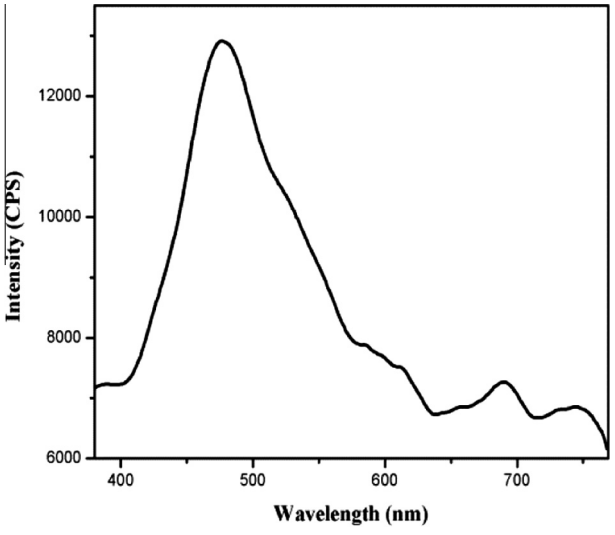

Figure 5 Fluorescence spectra of Co(II) complex.

3.6. Powder XRD and SEM

Powder XRD patterns of all the complexes were recorded over the 2θ = 10–80° range and all metal complexes display sharp crystalline peaks indicating their crystalline nature. It is also one of the evidences about the structure of the ligand and its complexes. The XRD patterns of the ligand and its Co(II) complex are shown in Fig. 6 and Fig. 7. Unit cell parameters were calculated by using trial and error methods as follows: all the compounds are triclinic with the unit cell parameters for ligand (L) compound: a = 9.1256 Å, b = 6.1933 Å, c = 5.6748 Å, α = 106.64°, β = 94.92°, γ = 100.60°,

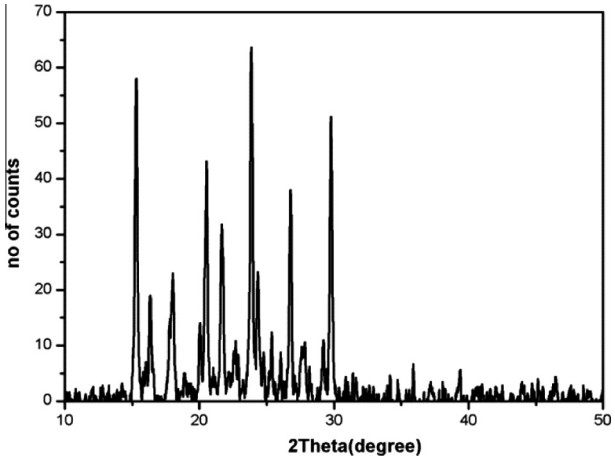

Figure 6 Powder XRD pattern of Ligand (L).

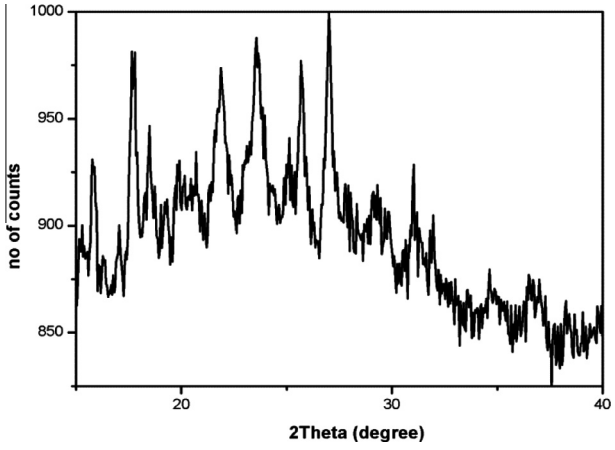

Figure 7 Powder XRD pattern of Co(II) complex.

$V = 320$ Å^3; for $[Cu(L)_2(H_2O)_2]$: $a = 9.3179$ Å, $b = 5.8284$ Å, $c = 5.7452$ Å, $\alpha = 105.8°$, $\beta = 97.21°$, $\gamma = 102.66°$, $V = 312$ Å^3; for $[Co(L)_2(H_2O)_2]$: $a = 8.7140$ Å, $b = 6.4951$ Å, $c = 5.4951$ Å, $\alpha = 108.26°$, $\beta = 97.55°$, $\gamma = 101.38°$, $V = 313$ Å^3; for $[Ni(L)_2(H_2O)_2]$: $a = 9.4561$ Å, $b = 6.6975$ Å, $c = 5.9236$ Å, $\alpha = 104.71°$, $\beta = 98.98°$, $\gamma = 100.61°$, $V = 376$ Å^3; for $[Zn(L)_2(H_2O)_2]\cdot 2H_2O$: $a = 9.2487$ Å, $b = 8.6127$ Å, $c = 5.4772$ Å, $\alpha = 107.94°$, $\beta = 99.07°$, $\gamma = 99.07°$, $V = 437$ Å^3. The average crystallite sizes (d_{XRD}) of the ligand and its Cu(II), Co(II), Ni(II) and Zn(II) complexes were calculated from Scherrer's formula (Warren, 1990) and were found to be 50, 30, 35, 30 and 42 nm, respectively.

The morphology and grain size of the metal complexes have been illustrated by the scanning electron micrograph (SEM). The SEM micrographs of all the metal complexes are shown in Fig. 8. For all the complexes the SEM micrographs were taken in the common scale of 20 μm. From the SEM micrographs it was noted that there is a uniform matrix in all the metal complexes. The micrograph of Cu(II) complex shows plate like morphology and the Co(II) complex shows small needle like morphology. Ni(II) and Zn(II) complexes show rod like morphology.

3.7. Antimicrobial activity

The antimicrobial activity of ligand (L) and its complexes are summarized in Table 5. The results are summarized in Table 5, are compared with those of the standard drug kanamycin for bacteria and clotrimazole for fungi. Metal complexes exhibit higher anti microbial activity than the free ligand against all the tested strains. The higher activity of metal complexes than that of the free ligand can be explained on the basis of Overtone's concept and chelation theory. On chelation, the polarity

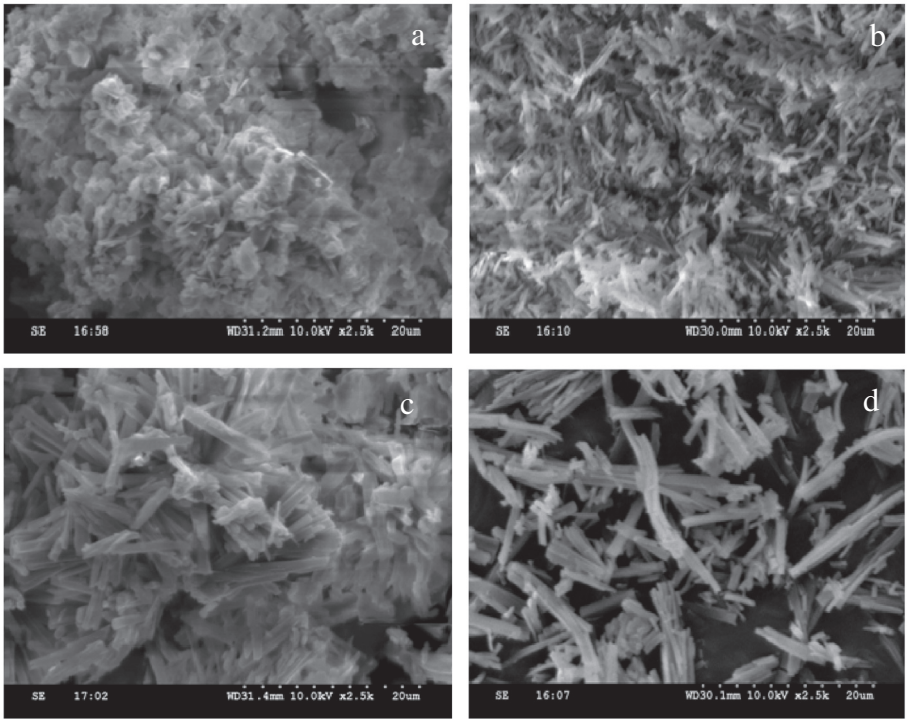

(a) [$Cu(L)_2(H_2O)_2$]; (b) $[Co(L)_2(H_2O)_2]$

(c) $[Ni(L)_2(H_2O)_2]$; (d) $[Zn(L)_2(H_2O)_2].2H_2O$

Figure 8 SEM micrographs of all metal complexes.

Table 5 MIC (μg/ml) values for antimicrobial activity of the ligand and its metal complexes.

Compound	*Bacillus subtilis*	*Staphylococcus aureus*	*Proteus vulgaris*	*Klebsiella pneumoniae*	*Candida albicans*
L	53	53	53	53	53
$[Cu(L)_2(H_2O)_2]$	45	45	45	48	50
$[Co(L)_2(H_2O)_2]$	30	30	30	30	35
$[Ni(L)_2(H_2O)_2]$	30	30	33	25	30
$[Zn(L)_2(H_2O)_2]\cdot 2H_2O$	45	45	45	45	48
Kanamycin	04	10	08	11	–
Clotrimazole	–	–	–	–	10

of the metal ion will be reduced to a greater extent due to the overlap of the ligand orbital and partial sharing of the positive charge of the metal ion with donor groups. Further, it increases the delocalization of π-electrons over the whole chelating ring and enhances the penetration of the complexes into lipid membranes and blocking of the metal binding sites in the enzymes of microorganisms. The other factors, which also increase the activity, are solubility, conductivity and bond length between the metal and ligand (Chohan et al., 2010).

3.8. Nematicidal activity

The nematicidal activity of the metal complexes is depicted in Table 6. So far, the chromones have been reported to have mostly pharmaceutical effects, but no information is available as to their nematicidal nature, hence the importance of the present finding. From the results, ligand alone does not show any nematicidal activity, but its metal complexes showed activity against the tested nematode that may be due to the chelation. All the metal complexes showed dose dependent nematicidal activity, i.e., when the concentration increases activity also increases. When the incubation time increases, all the metal complexes showed increased activity. Zn(II) complex showed greater activity when compared to the Cu(II), Co(II) and Ni(II) metal complexes.

3.9. DNA cleavage studies

Gel electrophoresis experiments using pUC19 were performed with the ligand and its complexes in the presence and absence of H_2O_2 as an oxidant. DNA cleavage is controlled by the relaxation of supercoiled circular form of pUC19 DNA into nicked circular form and linear form. When circular plasmid DNA is conducted by electrophoresis, the fastest migration will be observed for the supercoiled form (Form I). If one strand is cleaved, the supercoil will relax to produce a slower moving open circular form (Form II). If both strands are cleaved, a linear form (Form III) is generated, that migrates between Form I and Form II. The results (Fig. 9a) indicate that, in the absence of H_2O_2 all the compounds do not show cleavage activity but in the presence of an oxidising agent, the ligand and its metal complexes showed good DNA cleavage activity. In the Fig. 9b, Control (DNA + H_2O_2) does not show cleavage activity. The difference in migration observed in the lanes 1, 4, 5 of ligand and its Ni(II) and Zn(II) complexes, respectively, indicates the partial DNA cleavage. Lanes 2 and 3 clearly showed the absence of marker bands.

Table 6 Nematicidal activity (% mortality) values of metal complexes.

Compound	After 24 h			After 48 h		
	250 (μg/ml)	150 (μg/ml)	50 (μg/ml)	250 (μg/ml)	150 (μg/ml)	50 (μg/ml)
L	–	–	–	–	–	–
$[Cu(L)_2(H_2O)_2]$	27	19	6	38	28	13
$[Co(L)_2(H_2O)_2]$	18	10	5	28	18	11
$[Ni(L)_2.(H_2O)_2]$	45	28	13	62	44	22
$[Zn(L)_2.(H_2O)_2]\cdot 2H_2O$	48	31	16	65	48	26

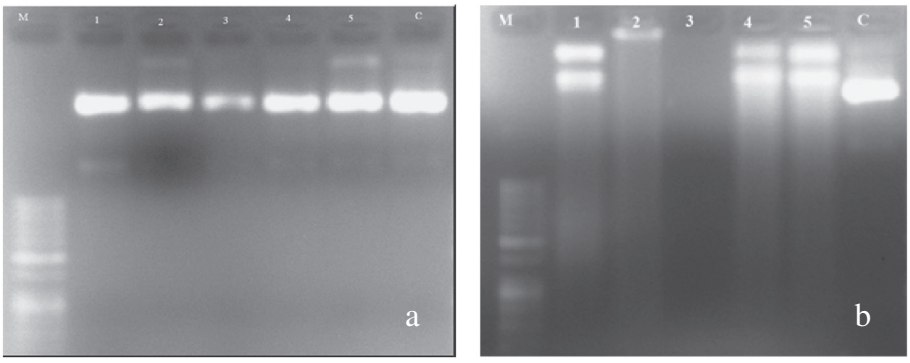

Fig a: In the absence of H_2O_2

Lane 1: DNA + Ligand; Lane 2: DNA + Cu(II) complex; Lane 3: DNA + Co(II) complex ; Lane 4: DNA + Ni(II) complex; Lane 5: DNA + Zn(II) complex; Lane C: Control(DNA alone).

Fig b: In the presence of H_2O_2

Lane 1: DNA + H_2O_2 + Ligand; Lane 2: DNA + H_2O_2 + Cu(II) complex; Lane 3: DNA + H_2O_2 + Co(II) complex ; Lane 4: DNA + H_2O_2 + Ni(II) complex; Lane 5: DNA + H_2O_2

Figure 9 Gel electrophoresis diagrams for DNA cleavage studies.

It indicates that the Cu(II) and Co(II) complexes showed complete DNA cleavage. Possible reaction mechanisms of DNA cleavage by the metal complexes in the presence of H_2O_2 have been reported by several research groups (Yamamoto and Kawanishi, 1989; Dominique et al., 2012).

4. Conclusions

In the present work, Cu(II), Co(II), Ni(II) and Zn(II) complexes were prepared from 3-formyl chromone Schiff base and are characterised using various spectral techniques. The IR spectral data demonstrate that the ligand acts as bidentate, coordinating through azomethane nitrogen and carbonyl oxygen atoms. Thermal data provided the number of coordinated and lattice water molecules in the complexes. Magnetic and Electronic spectral studies revealed octahedral geometry for all the metal complexes. From the ESR spectra tetragonally distorted octahedral geometry was confirmed for the Cu(II) complex. All metal complexes exhibit fluorescence. Powder XRD results show that the ligand and its complexes are crystalline in nature. SEM analysis of all metal complexes revealed their homogeneous nature. The antimicrobial and nematicidal activities clearly indicated that the metal complexes exhibited greater activity than the ligand. The ligand and its metal complexes showed DNA cleavage activity in the presence of H_2O_2.

Acknowledgements

Authors wish to thank Professor B. Viswanathan, NCCR, and the IIT Madras for recording fluorescence spectra. Authors would like to express thanks to the IIT Hyderabad for generously providing TG facility and the Vimta Labs Hyderabad for DNA cleavage studies.

References

Aazam, E.S., EL Husseiny, A.F., Al-Amri, H.M., 2012. Arabian J. Chem. 5, 45–53.
Athanasellis, G., Melagraki, G., Afantitis, A., Makridima, K., IgglessiMarkopoulou, O., 2006. Arkivoc 10, 28–34.
Barve, Vivek, Ahmed, Fakhara, Adsule, Shreelekha, Banerjee, Sanjeev, 2006. Eur. J. Med. Chem. 49, 3800–3808.
Carmona, P., Molina, M., Escobar, R., 1993. Spectrochim. Acta, Part A 49 (1), 1–9.
Cayrol, J., Djian, C., Pijarowski, L., 1989. Rev. Nematologie 12 (4), 331–336.
Chohan, Z.H., Iqbal, M.S., Aftab, S.K., 2010. Appl. Organomet. Chem. 24, 47–56.
David, S.S., Williams, S.D., 1998. Chem. Rev. 98, 1221–1261.
Dega-Szafran, Z., Kania, A., Nowak-Wyadra, B., Szafran, M., 1994. J. Mol. Struct. 322, 223–232.
Dominique, Desbouisa, Troitsky, Ivan P., Belousoff, Matthew J., Spiccia, Leone, Bim, Graham, 2012. Coord. Chem. Rev. 256, 897–937.
Ellis, G.P., 1977. The Chemistry of Heterocyclic Compounds. Wiley, New York, vol. 31, p. 749.
Fuhrmann, H., Brenner, S., Arndt, P., 1996. Inorg. Chem. 35, 6742–6745.
Geary, W., 1971. J. Coord. Chem. Rev. 7, 81–122.
Ghosh, Kaushik, Kumar, Pramod, Tyagi, Nidhi, 2011. Inorg. Chim. Acta 375, 77–83.
Hathaway, B.J., 1984. Struct. Bonding (Berlin) 57, 55–118.
Hathaway, B.J., Billing, D.E., 1970. Coord. Chem. Rev. 5, 143–207.
Jain, M., Maanju, S., Singh, R.V., 2004. Appl. Organomet. Chem. 18, 73–82.
Kapoor, Puja, Singh, R.V., Fahmi, Nighat, 2012. J. Coord. Chem. 65 (2), 262–277.
Kivelson, D., Neiman, R., 1961. J. Chem. Phys. 35, 149–155.
Li, Y., Yang, Z.Y., Liao, Z.C., Han, Z.C., Liu, Z.C., 2010a. Inorg. Chem. Commun. 13, 1213–1216.
Li, Y., Yang, Z.Y., Wu, J.C., 2010b. Eur. J. Med. Chem. 45, 5692–5701.
Liu, J., Zhang, T., Lu, T., Qu, L., Zhou, H., Zhang, Q., Ji, L., 2002. J. Inorg. Biochem. 91, 269–276.
Lu, Z.L., Duan, C.Y., Tian, Y.P., You, X.Z., 1996. Inorg. Chem. 35, 2253–2258.
McWhinnie, W.R., 1964. J. Chem. Soc., 2959–2969.
Ng, C.H., Kong, K.C., Von, S.T., Balraj, P., Jensen, P., Thirthagiri, E., Hamada, H., Chikira, M., 2000. Nucleic Acids Res. 28, 4856–4864.
Nickless, D.E., Power, M.J., Urbach, F.N., 1983. Inorg. Chem. 22, 3210–3217.
Nohara, Akira, Umetani, Tomonobu, Sanno, Yasushi, 1973. Tetrahedron Lett. 14 (22), 1995–1998.
Okamato, M., Takahashi, K., Doi, T., Takimoto, Y., 1997. Anal. Chem. 69, 2919–2926.
Parvatha, R.P., Khan, R.M., 1991. Curr. Nematolog. 2, 115.
Piao, L.Z., Park, H.R., Park, Y.K., Lee, S.K., Park, J.H., Park, M.K., 2002. Chem. Pharm. Bull. 50, 309–311.
Qin, D.D., Yang, Z.Y., Wang, B.D., 2007. Spectrochim. Acta, Part A 68, 912–917.
Raman, N., Ravichandran, S., Thangaraja, C., 2004. J. Chem. Sci. 116, 215–219.
Reddy, P.R., Rao, K.S., Satyanarayana, B., 2006. Tetrahedron Lett. 47, 7311–7315.
Sancar, A., Sancar, G.B., 1988. Annu. Rev. Biochem. 57, 29–67.
Shukla, P.R., Singh, V.K., Jaiswal, A.M., Narain, J., 1983. J. Indian Chem. Soc. 60, 321–324.
Singh, G.R., Singh, N.K., Girdhar, M.P., Ishar, S., 2002a. Tetrahedron 58, 2471–2480.
Singh, G., Singh, P.A., Singh, K., Singh, D.P., Handa, R.N., Dubey, S.N., 2002b. Proc. Natl. Acad. Sci. India 72A, 87–94.
Singh, O.I., Damayanti, M., Singh, N.R., Singh, R.K.H., Mohapatra, M., Kadam, R.M., 2005. Polyhedron 24, 909–916.
Solomon, E.I., Baldwin, M.J., Lowery, M.D., 1992. Chem. Rev. 92, 521–542.
Suksrichavalit, T., Prachayasittikul, S., Nantasenamat, C., Isarankura-Na-Ayudhya, C., Prachayasittikul, V., 2009. Eur. J. Med. Chem. 44, 3259–3265.
Teimouri, Mohammed Bagher, 2011. Tetrahedron 67, 1837–1843.
Vaidyanathan, V.G., Nair, B.U., 2003. J. Inorg. Biochem. 93, 271–276.
Walenzyk, T., carola, C., Buchholzb, H., koniga, B., 2005. Tetrahedron 61, 7366–7377.
Wang, Ju, Yang, Zheng-Yin, Yi, Xu-Yang, Wang, Bao-Dui, 2009. J. Photochem. Photobiol., A 201, 183–190.
Wang, B.D., Yang, Z.Y., Hua Lu, M., Hai, J., Hai, J., Wang, Q., Chen, Z.N., 2009. J. Organomet. Chem. 694, 4069–4075.
Warren, B.E., 1990. X-ray Diffraction, second ed. Dover, New York.
Ya Sosnovskikh, V., 2003. Russ. Chem. Rev. 72, 489–516.
Yamamoto, K., Kawanishi, S., 1989. J. Biol. Chem. 264, 15435–15440.